AIAA JOURNAL
Vol. 45, No. 11, November 2007

Stress Analysis of Functionally Graded Thick-Walled Cylindrical Vessels

L. H. You*
Chongqing University, 400044 Chongqing City, People's Republic of China
H. Ou†
Queen's University Belfast, Belfast, Northern Ireland BT9 5AH, United Kingdom
and
Jun Li‡
Chongqing University, 400044 Chongqing City, People's Republic of China

DOI: 10.2514/1.31926

In this paper, a simple and accurate method is presented to determine deformations and stresses in thick-walled cylindrical vessels made of functionally graded materials under internal pressure and uniform temperature. The governing equation with the consideration of varying Young's modulus and thermal expansion coefficient along the radial direction is derived from the basic equations of axisymmetric plane strain problems in elasticity. The comparison with the corresponding numerical solution indicates that the proposed solution has excellent convergence and accuracy. The effects of the coefficients, which affect Young's modulus and the thermal expansion coefficient, on the deformation and stresses in thick-walled cylindrical vessels are investigated.

Nomenclature

a_1, a_2, b_j, c_j	=	unknown constants
c, d	=	constants
E	=	Young's modulus of functionally graded material
E_i	=	Young's modulus of functionally graded material at r_i
E_j	=	Young's modulus of the jth concentric circular ring
$E_{\mathrm{Ni}}, E_{\mathrm{TiC}}$	=	Young's moduli of Ni and TiC
e_0, e_1, e_2	=	coefficients determining the variation of Young's modulus
$H(c,d,z)$, $I(c,d,z)$	=	independent solutions
$J(c,d,z)$, $K(c,d,z)$, $L(c,d,z)$	=	unknown functions
M	=	compositional distribution exponent
N	=	total number of concentric circular rings
p	=	applied internal pressure
q	=	constant
r	=	radial coordinate
r_i, r_o	=	inner and outer radii of the cylindrical vessel
r_j	=	inner radius of the jth concentric circular ring
u	=	radial displacement
$\bar{u}$	=	dimensionless radial displacement
u^j	=	radial displacement of the jth concentric circular ring
$V_{\mathrm{Ni}}, V_{\mathrm{TiC}}$	=	volume fractions of Ni and TiC
$v_1(c,d,z)$, $v_2(c,d,z)$	=	unknown functions
z	=	variable related to the radial coordinate r
z_1	=	value of variable z at the radial coordinate r_i
α	=	thermal expansion coefficient of functionally graded material
α_j	=	thermal expansion coefficient of the jth concentric circular ring
$\alpha_{\mathrm{Ni}}, \alpha_{\mathrm{TiC}}$	=	thermal expansion coefficients of Ni and TiC
$\alpha_0, \alpha_1, \alpha_2$	=	coefficients determining the change of the thermal expansion coefficient
Δr	=	thickness of each concentric circular ring
ΔT	=	uniform temperature change
$\varepsilon_r, \varepsilon_\theta, \varepsilon_z$	=	radial, circumferential, and axial strains
ν	=	Poisson's ratio
ν_j	=	Poisson's ratio of the jth concentric circular ring
ξ	=	stress–strain transfer ratio
$\sigma_r, \sigma_\theta, \sigma_z$	=	radial, circumferential, and axial stresses
$\tilde{\sigma}_r, \tilde{\tilde{\sigma}}_r$	=	complementary solution and particular solution
$\bar{\sigma}_r, \bar{\sigma}_\theta, \bar{\sigma}_z$	=	dimensionless radial, circumferential, and axial stresses
$\sigma_r^j, \sigma_\theta^j, \sigma_z^j$	=	radial, circumferential, and axial stresses in the jth concentric circular ring
σ_r^1, σ_r^N	=	radial stress at the inner and outer radii of the cylindrical vessel, respectively

Received 3 May 2007; revision received 16 July 2007; accepted for publication 16 July 2007.

*Senior Research Fellow, The State Key Laboratory of Mechanical Transmission.
†Lecturer, School of Mechanical and Aerospace Engineering.
‡Associate Professor, College of Mechanical Engineering.

Introduction

AS A basic form of structural components widely used in many engineering applications, accurate prediction of deformation and stresses of thick-walled cylindrical vessels is essential to ensure specified performance requirements under various mechanical and thermal loading conditions. In past decades, solutions to elastic behavior of thick-walled cylindrical vessels were well-established, particularly for homogenous materials. In recent years, research interests have been focused on elastic–plastic analysis methods in evaluating thick-walled cylindrical vessels. Using Tresca's yield criterion, Bland [1] obtained the solution of stresses, strains, and displacements in a thick-walled tube with working-hardening material subjected to internal and external pressures and different temperatures. With Hencky's deformation theory and von Mises's yield criterion, Gao [2] derived a closed-form analytical solution to determine displacements, strains, and stresses in an internally pressurized open-ended thick-walled cylinder made of a strain-hardening material. By introducing large strain theory, it was also

possible to obtain an exact elastoplastic analytical solution of thick-walled cylinders under internal pressure [3]. Modeling material behavior by a finite strain elastoplastic flow theory, Durban and Kubi [4] presented a general solution of pressurized elastoplastic tubes. Using a rate-independent plasticity theory and including kinematic and isotropic hardening effects, Bonn and Haupt [5] developed an exact solution to describe finite elastic–plastic deformations and stresses in thick-walled tubes. Sayir and Motavalli [6] investigated stress and deformation fields in a fiber-reinforced composite tube under uniform internal pressure. Kandil et al. [7] proposed a numerical approach to analyze thermal stresses within a thick-walled cylinder under dynamic internal temperature gradient. With a numerical model based on forward finite difference technique, Kandil [8] also determined time-dependent stress distributions in thick-walled cylindrical pressure vessels subjected to cyclic internal pressure and temperature. Based on a second-gradient elastoplastic model developed to regularize the ill-posedness caused by material strain softening behavior, Zervos et al. [9] modeled the progressive localization of deformation in thick-walled cylinders. Zhao et al. [10] presented a technique involving two parametric functions and piecewise linearization of the stress–strain curve to carry out elastic–plastic analysis of a thick-walled elastic–plastic cylinder.

With the advantage of spatially distributed material properties for enhanced performance particularly in thermal properties, corrosion, and fracture resistance, functionally graded materials have been increasingly used in the design and construction of thick-walled cylindrical vessels for different applications. Because of this reason, research into functionally graded structural components such as cylindrical vessels has been reported more frequently in recent years. For example, Finot and Suresh [11] examined effects of layer geometry, plastic flow, and compositional gradation on small and large deformations in multilayered materials during temperature excursions. Afsar and Sekine [12] proposed a solution method to evaluate optimum material distributions for prescribed apparent fracture toughness in thick-walled functionally graded material circular pipes. Ma and Wang [13] investigated axisymmetric large deflection bending and postbuckling of a functionally graded circular plate under mechanical and thermal loadings. Liew et al. [14] presented an analysis of thermomechanical behavior of hollow circular cylinders made of functionally graded materials. Chen [15] performed elastic calculations of a cracked cylinder of functionally graded materials. You et al. [16] carried out elastic analysis of thick-walled spherical pressure vessels consisting of functionally graded material systems subjected to internal pressure.

Because of varying material properties, the governing equations describing deformation and stresses of functionally graded thick-walled cylindrical vessels are difficult to solve analytically. Partitioning the cylinder into a series of concentric circular rings is a common approach to obtain approximate solutions through numerical computation. Because of the requirement for data preparation and program implementation, such a procedure may not be the most attractive or efficient for design evaluation and validation purposes. Therefore, in this paper, we develop a simple and accurate solution to predict the deformations and stresses occurring in functionally graded cylindrical vessels under internal pressure and uniform temperature change. Such an approach is useful for engineering problems, especially at the preliminary design stage. To achieve this, first we start with the basic theory of axisymmetric elastic deformation under plane strain conditions to develop an analytical solution for a nonhomogenous second-order ordinary differential equation. We then verify the derived analytical solution with numerical results of a cylindrical vessel made of a particular functionally graded material. Finally, we examine how different material properties affect deformation and stresses in functionally graded thick-walled cylindrical vessels subjected to internal pressure and uniform temperature change.

Basic Equations and Analytical Solution

When subjected to an internal pressure, under uniform temperature conditions, the deformation of the cylindrical vessel is assumed axisymmetric. When the cylindrical vessels are long enough, the plane strain condition may be assumed as well. Therefore, there is only a radial displacement component in the cylindrical vessels, which results in radial and circumferential strain components and radial, circumferential, and axial stress components. For most functionally graded materials, the material properties such as Young's modulus and thermal expansion coefficient are a function of composition distribution. In this paper, both of the material properties are expressed by exponential functions of the radial coordinate of the thick-walled cylinder. For many engineering materials, Poisson's ratio is within the range from 0.25 to 0.35 and the variation in value is relatively small. Thus, Poisson's ratio is assumed to be constant and an average value is taken in this paper.

In thick-walled cylindrical vessels under internal pressure and uniform temperature change, the total radial, circumferential, and axial strains in the cylindrical vessel can be described by the following equations:

$$\varepsilon_r = \tfrac{1}{E}[\sigma_r - \nu(\sigma_\theta + \sigma_z)] + \alpha\Delta T \tag{1a}$$

$$\varepsilon_\theta = \tfrac{1}{E}[\sigma_\theta - \nu(\sigma_r + \sigma_z)] + \alpha\Delta T \tag{1b}$$

$$\varepsilon_z = \tfrac{1}{E}[\sigma_z - \nu(\sigma_r + \sigma_\theta)] + \alpha\Delta T \tag{1c}$$

With the assumption of the plane strain condition, the axial strain disappears (i.e., $\varepsilon_z = 0$). Substituting it into Eq. (1c), the axial stress may be expressed in terms of radial and circumferential stresses as follows:

$$\sigma_z = \nu(\sigma_r + \sigma_\theta) - E\alpha\Delta T \tag{2}$$

Substituting the preceding equation into Eqs. (1a) and (1b), the relations between the strains and stresses become

$$\begin{aligned} \varepsilon_r &= \tfrac{1}{E}[(1-\nu^2)\sigma_r - \nu(1+\nu)\sigma_\theta] + (1+\nu)\alpha\Delta T \\ \varepsilon_\theta &= \tfrac{1}{E}[(1-\nu^2)\sigma_\theta - \nu(1+\nu)\sigma_r] + (1+\nu)\alpha\Delta T \end{aligned} \tag{3}$$

Because of the axisymmetric deformations, the stresses in thick-walled cylindrical vessels are also axisymmetric. The stress equilibrium equation can be written as

$$\sigma_\theta = \sigma_r + r\frac{\mathrm{d}\sigma_r}{\mathrm{d}r} \tag{4}$$

Substituting Eq. (4) into Eq. (3), the radial and circumferential strains are represented in terms of the radial stress using the following equations:

$$\begin{aligned} \varepsilon_r &= \frac{1+\nu}{E}\left[(1-2\nu)\sigma_r - \nu r\frac{\mathrm{d}\sigma_r}{\mathrm{d}r}\right] + (1+\nu)\alpha\Delta T \\ \varepsilon_\theta &= \frac{1+\nu}{E}\left[(1-2\nu)\sigma_r + (1-\nu)r\frac{\mathrm{d}\sigma_r}{\mathrm{d}r}\right] + (1+\nu)\alpha\Delta T \end{aligned} \tag{5}$$

The preceding radial and circumferential strains are related to the radial displacement through the following geometric relationships:

$$\varepsilon_r = \frac{\mathrm{d}u}{\mathrm{d}r}, \qquad \varepsilon_\theta = \frac{u}{r} \tag{6}$$

The deformation compatibility equation is reached by eliminating the radial displacement u from the preceding equation and has the form of

$$r\frac{\mathrm{d}\varepsilon_\theta}{\mathrm{d}r} + \varepsilon_\theta - \varepsilon_r = 0 \tag{7}$$

For functionally graded cylindrical vessels, the material properties are functions of the radial coordinate r. Substituting Eq. (5) into Eq. (7) and taking into account the variations of Young's modulus and thermal expansion coefficient along the radial direction, the

governing equation, in terms of radial stress and its first derivative, is found to be

$$r\frac{\mathrm{d}^2\sigma_r}{\mathrm{d}r^2}+\left(3-\frac{r}{E}\frac{\mathrm{d}E}{\mathrm{d}r}\right)\frac{\mathrm{d}\sigma_r}{\mathrm{d}r}-\frac{1-2\nu}{(1-\nu)E}\frac{\mathrm{d}E}{\mathrm{d}r}\sigma_r+\frac{E}{1-\nu}\Delta T\frac{\mathrm{d}\alpha}{\mathrm{d}r}=0 \tag{8}$$

Equation (8) can be solved by using numerical methods such as that given in [17]. For some specific variations of Young's modulus and thermal expansion coefficient, Eq. (8) can be solved analytically.

There have been some assumed variations of material properties for functionally graded materials in existing literature [11]. Here, we use the following equations to describe the variations of Young's modulus and the thermal expansion coefficients of cylindrical vessels:

$$E=e_0e^{e_1+e_2r},\qquad \alpha=\alpha_0e^{\alpha_1+\alpha_2r} \tag{9}$$

Substituting Eq. (9) into Eq. (8), the following nonhomogeneous second-order ordinary differential equation is obtained:

$$r\frac{\mathrm{d}^2\sigma_r}{\mathrm{d}r^2}+(3-e_2r)\frac{\mathrm{d}\sigma_r}{\mathrm{d}r}-\frac{1-2\nu}{1-\nu}e_2\sigma_r+\frac{e_0\alpha_0\alpha_2}{1-\nu}e^{e_1+\alpha_1+(e_2+\alpha_2)r}\Delta T=0 \tag{10}$$

Introducing a new variable, z,

$$z=e_2r \tag{11}$$

Equation (10) is transformed into

$$\frac{\mathrm{d}^2\sigma_r}{\mathrm{d}z^2}+\frac{d-z}{z}\frac{\mathrm{d}\sigma_r}{\mathrm{d}z}-\frac{c}{z}\sigma_r=-\frac{e_0\alpha_0\alpha_2}{(1-\nu)e_2z}e^{e_1+\alpha_1+\frac{e_2+\alpha_2}{e_2}z}\Delta T \tag{12}$$

where

$$d=3,\qquad c=\frac{1-2\nu}{1-\nu} \tag{13}$$

One independent solution of the associated homogeneous differential equation of Eq. (12) is [18]

$$H(c,d,z)=(c)_0+\frac{(c)_1}{(d)_1}z+\frac{(c)_2}{2!(d)_2}z^2+\frac{(c)_3}{3!(d)_3}z^3+\cdots+\frac{(c)_n}{n!(d)_n}z^n+\cdots \tag{14}$$

where

$$(q)_0=1,\qquad (q)_n=q(q+1)(q+2)+\cdots+(q+n-1)\quad(q=c,d;n=1,2,3,\ldots) \tag{15}$$

According to the theory of second-order ordinary differential equations, the other independent solution of the associated homogeneous differential equation of Eq. (12) can be constructed as

$$I(c,d,z)=H(c,d,z)J(c,d,z) \tag{16}$$

where

$$J(c,d,z)=\int_{z_1}^{z}\frac{z^{-d}e^z}{H^2(c,d,z)}\,\mathrm{d}z \tag{17}$$

and $z_1=e_2r_i$.

The complementary solution of the associated homogeneous differential equation of Eq. (12) is a linear combination of the preceding two independent solutions; that is,

$$\tilde{\sigma}_r=H(c,d,z)[a_1+a_2J(c,d,z)] \tag{18}$$

The particular solution of nonhomogeneous second-order ordinary differential equation (12) can be constructed as

$$\tilde{\tilde{\sigma}}_r=v_1(c,d,z)H(c,d,z)+v_2(c,d,z)I(c,d,z) \tag{19}$$

In Eq. (19), $v_1(c,d,z)$ and $v_2(c,d,z)$ are two unknown functions that can be determined by the following two equations:

$$\frac{\mathrm{d}v_1(c,d,z)}{\mathrm{d}z}=\frac{I(c,d,z)}{H(c,d,z)I'(c,d,z)-I(c,d,z)H'(c,d,z)}\frac{e_0\alpha_0\alpha_2}{(1-\nu)e_2z}\times e^{e_1+\alpha_1+\frac{e_2+\alpha_2}{e_2}z}\Delta T$$
$$\frac{\mathrm{d}v_2(c,d,z)}{\mathrm{d}z}=-\frac{H(c,d,z)}{H(c,d,z)I'(c,d,z)-I(c,d,z)H'(c,d,z)}\frac{e_0\alpha_0\alpha_2}{(1-\nu)e_2z}\times e^{e_1+\alpha_1+\frac{e_2+\alpha_2}{e_2}z}\Delta T \tag{20}$$

where

$$H'(c,d,z)=\frac{\mathrm{d}H(c,d,z)}{\mathrm{d}z}=\frac{c}{d}H(c+1,d+1,z)$$
$$J'(c,d,z)=\frac{\mathrm{d}J(c,d,z)}{\mathrm{d}z}=\frac{z^{-d}e^z}{H^2(c,d,z)}$$
$$I'(c,d,z)=\frac{\mathrm{d}I(c,d,z)}{\mathrm{d}z}=\frac{c}{d}H(c+1,d+1,z)J(c,d,z)+\frac{z^{-d}e^z}{H(c,d,z)} \tag{21}$$

Substituting Eq. (21) into Eq. (20) and integrating from z_1 to z, the unknown functions $v_1(c,d,z)$ and $v_2(c,d,z)$ are described in the following equation:

$$v_1(c,d,z)=\frac{e_0\alpha_0\alpha_2\Delta T}{(1-\nu)e_2}\int_{z_1}^{z}H(c,d,z)z^{d-1}e^{e_1+\alpha_1+\frac{\alpha_2}{e_2}z}J(c,d,z)\mathrm{d}z$$
$$v_2(c,d,z)=-\frac{e_0\alpha_0\alpha_2\Delta T}{(1-\nu)e_2}\int_{z_1}^{z}H(c,d,z)z^{d-1}e^{e_1+\alpha_1+\frac{\alpha_2}{e_2}z}\mathrm{d}z \tag{22}$$

Substituting Eq. (22) into Eq. (19) and introducing notations

$$K(c,d,z)=\int_{z_1}^{z}H(c,d,z)z^{d-1}e^{e_1+\alpha_1+\frac{\alpha_2}{e_2}z}\mathrm{d}z$$
$$L(c,d,z)=\int_{z_1}^{z}H(c,d,z)z^{d-1}e^{e_1+\alpha_1+\frac{\alpha_2}{e_2}z}J(c,d,z)\mathrm{d}z \tag{23}$$

the particular solution of Eq. (12) is obtained and has the form of

$$\tilde{\tilde{\sigma}}_r=\frac{e_0\alpha_0\alpha_2\Delta T}{(1-\nu)e_2}H(c,d,z)[L(c,d,z)-J(c,d,z)K(c,d,z)] \tag{24}$$

Superimposing Eq. (24) on Eq. (18) and making use of Eq. (11), the general solution of nonhomogeneous second-order ordinary differential equation (12) is found to be

$$\sigma_r=H(c,d,e_2r)\left\{a_1+a_2J(c,d,e_2r)+\frac{e_0\alpha_0\alpha_2\Delta T}{(1-\nu)e_2}[L(c,d,e_2r)-J(c,d,e_2r)K(c,d,e_2r)]\right\} \tag{25}$$

Substituting Eq. (25) into Eq. (4), the circumferential stress is determined by

$$\sigma_\theta = a_1\left[H(c,d,e_2r) + \frac{ce_2r}{d}H(c+1,d+1,e_2r)\right] + a_2\{J(c,d,e_2r)\left[H(c,d,e_2r) + \frac{ce_2r}{d}H(c+1,d+1,e_2r)\right] + \frac{(e_2r)^{1-d}e^{e_2r}}{H(c,d,e_2r)}\Big\} + \frac{e_0\alpha_0\alpha_2\Delta T}{(1-\nu)e_2}\left\{\left[H(c,d,e_2r) + \frac{ce_2r}{d}H(c+1,d+1,e_2r)\right][L(c,d,e_2r) - J(c,d,e_2r)K(c,d,e_2r)] - \frac{(e_2r)^{1-d}e^{e_2r}}{H(c,d,e_2r)}K(c,d,e_2r)\right\} \quad (26)$$

Substituting the radial stress equation (25), the circumferential stress equation (26), and material properties equation (9) into Eq. (2), the axial stress is written as

$$\sigma_z = a_1\nu\left[2H(c,d,e_2r) + \frac{ce_2r}{d}H(c+1,d+1,e_2r)\right] + a_2\nu\{J(c,d,e_2r)\left[2H(c,d,e_2r) + \frac{ce_2r}{d}H(c+1,d+1,e_2r)\right] + \frac{(e_2r)^{1-d}e^{e_2r}}{H(c,d,e_2r)}\Big\} + \frac{\nu e_0\alpha_0\alpha_2\Delta T}{(1-\nu)e_2}\left\{\left[2H(c,d,e_2r) + \frac{ce_2r}{d}H(c+1,d+1,e_2r)\right][L(c,d,e_2r) - J(c,d,e_2r)K(c,d,e_2r)] - \frac{(e_2r)^{1-d}e^{e_2r}}{H(c,d,e_2r)}K(c,d,e_2r)\right\} - e_0\alpha_0\Delta T e^{e_1+\alpha_1+(e_2+\alpha_2)r} \quad (27)$$

Substituting Eqs. (25–27) into Eq. (1b), the circumferential strain is obtained. Substituting it into the second equation of Eq. (6), the radial displacement is given by

$$u = \frac{(1+\nu)r}{e_0e^{e_1+e_2r}}\left\{a_1\left[(1-2\nu)H(c,d,e_2r) + (1-\nu)\frac{ce_2r}{d}H(c+1,d+1,e_2r)\right] + a_2\left[\left((1-2\nu)H(c,d,e_2r) + (1-\nu)\frac{ce_2r}{d}H(c+1,d+1,e_2r)\right)J(c,d,e_2r) + (1-\nu)\frac{(e_2r)^{1-d}e^{e_2r}}{H(c,d,e_2r)}\right] + \frac{e_0\alpha_0\alpha_2\Delta T}{(1-\nu)e_2}\left[\left((1-2\nu)H(c,d,e_2r) + (1-\nu)\frac{ce_2r}{d}H(c+1,d+1,e_2r)\right)(L(c,d,e_2r) - J(c,d,e_2r)K(c,d,e_2r)) - (1-\nu)\frac{(e_2r)^{1-d}e^{e_2r}}{H(c,d,e_2r)}K(c,d,e_2r)\right]\right\} + (1+\nu)\alpha_0\Delta Tre^{\alpha_1+\alpha_2r} \quad (28)$$

Subject to internal pressure and uniform temperature change, the boundary conditions of thick-walled cylindrical vessels are

$$r = r_i, \qquad \sigma_r = -p, \qquad r = r_o, \qquad \sigma_r = 0 \quad (29)$$

Introducing Eq. (25) into Eq. (29) and solving for the unknown constants a_1 and a_2, the following equations are obtained:

$$a_1 = -\frac{p}{H(c,d,e_2r_i)}$$
$$a_2 = \left\{p - \frac{e_0\alpha_0\alpha_2\Delta T}{(1-\nu)e_2}H(c,d,e_2r_i)[L(c,d,e_2r_o) - J(c,d,e_2r_o)K(c,d,e_2r_o)]\right\}[H(c,d,e_2r_i)J(c,d,e_2r_o)]^{-1} \quad (30)$$

Substituting a_1 and a_2 into Eqs. (25–28), all stresses and radial displacement in thick-walled cylindrical vessels are determined.

To examine the correctness of the proposed approach, a simple numerical method is briefly introduced here. First, we uniformly divide a thick-walled cylindrical vessel into N concentric circular rings. Young's modulus and thermal expansion coefficient of each ring are assumed to be constants and taken from the middle of the ring. Because $(\mathrm{d}E/\mathrm{d}r) = (\mathrm{d}\alpha/\mathrm{d}r) = 0$ for each ring, Eq. (8) becomes

$$r\frac{\mathrm{d}^2\sigma_r}{\mathrm{d}r^2} + 3\frac{\mathrm{d}\sigma_r}{\mathrm{d}r} = 0 \quad (31)$$

Solving Eq. (31), the radial stress is obtained. The circumferential and axial stresses are determined by Eqs. (2) and (4), respectively. Then, the radial displacement can be derived from Eqs. (1) and (6). For the jth ring, these quantities have the forms of

$$\begin{aligned}&\sigma_r^j = -0.5b_jr^{-2} + c_j, \qquad \sigma_\theta^j = 0.5b_jr^{-2} + c_j\\ &\sigma_z^j = 2\nu_jc_j - E_j\alpha_j\Delta T\\ &u^j = \frac{1+\nu_j}{E_j}[0.5b_jr^{-1} + (1-2\nu_j)c_jr] + (1+\nu_j)\alpha_j\Delta Tr\end{aligned} \quad (32)$$

The boundary conditions of thick-walled cylindrical vessels and the continuity conditions of radial displacement and stress between adjacent rings are

$$\begin{aligned}&r = r_i, \qquad \sigma_r^1 = -p, \qquad r = r_j, \qquad \sigma_r^j = \sigma_r^{j+1}, \qquad u^j = u^{j+1}\\ &r = r_o, \qquad \sigma_r^N = 0 \qquad (j = 1,2,3,\cdots,N-1)\end{aligned} \quad (33)$$

where

$$r_j = r_i + j\Delta r, \qquad \Delta r = \frac{r_o - r_i}{N} \quad (34)$$

Substituting Eq. (32) into Eq. (33), $2N$ linear algebraic equations are obtained and the solution to the $2N$ linear algebraic equations will determine the $2N$ unknown constants b_j and c_j in Eq. (32).

Numerical Applications

A thick-walled cylindrical vessel made of a TiC–Ni functionally graded material under an internal pressure of 200 MPa and a uniform temperature change of 500°C is considered here. The inner and outer radii of the cylindrical vessel are 0.3 and 0.5 m, respectively. Young's modulus, Poisson's ratio, and the thermal expansion coefficient are 460 GPa, 0.336, and 7.4×10^{-6}/K for TiC and 199.5 GPa, 0.312, and 18×10^{-6}/K for Ni, respectively [19]. The thermal expansion coefficient and Young's modulus of the TiC–Ni functionally graded material are determined by the following rule of mixtures and empirical modified law of mixtures [19,20], respectively,

$$\begin{aligned}&\alpha = \alpha_{\mathrm{Ni}}V_{\mathrm{Ni}} + \alpha_{\mathrm{TiC}}V_{\mathrm{Tic}}\\ &E = \frac{[(\xi + E_{\mathrm{TiC}})/(\xi + E_{\mathrm{Ni}})V_{\mathrm{Ni}}E_{\mathrm{Ni}} + V_{\mathrm{TiC}}E_{\mathrm{TiC}}]}{[(\xi + E_{\mathrm{TiC}})/(\xi + E_{\mathrm{Ni}})V_{\mathrm{Ni}} + V_{\mathrm{TiC}}]}\end{aligned} \quad (35)$$

where

$$V_{\mathrm{Ni}} = \left(\frac{r - r_i}{r_o - r_i}\right)^M, \qquad V_{\mathrm{Tic}} = 1 - V_{\mathrm{ni}} \quad (36)$$

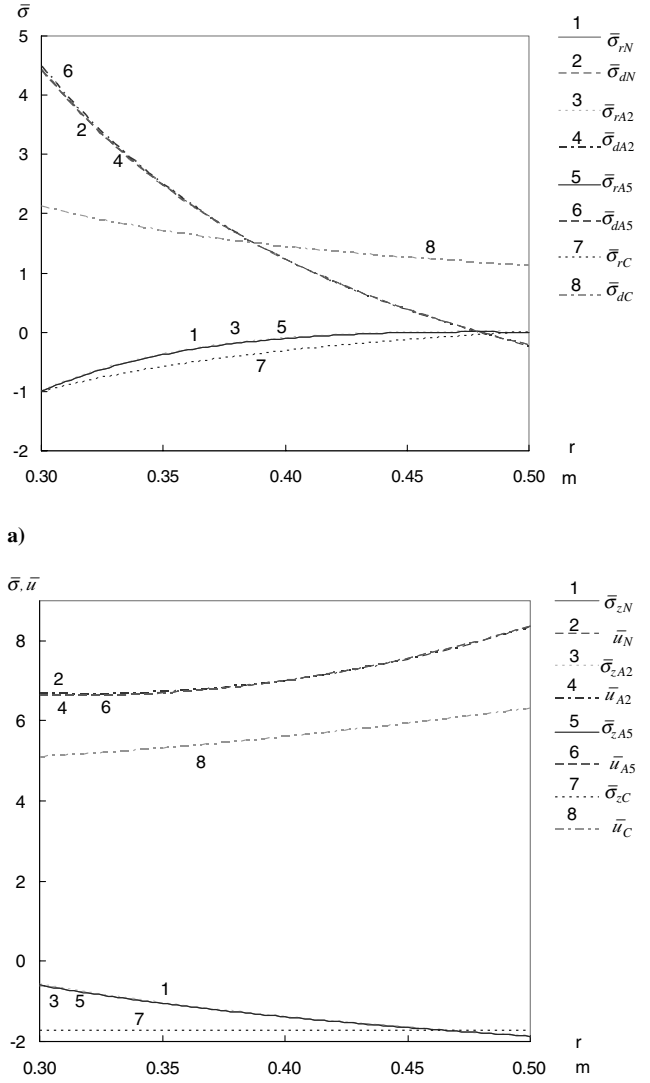

Fig. 1 Comparison of a) radial and circumferential stresses and b) axial stress and radial displacement.

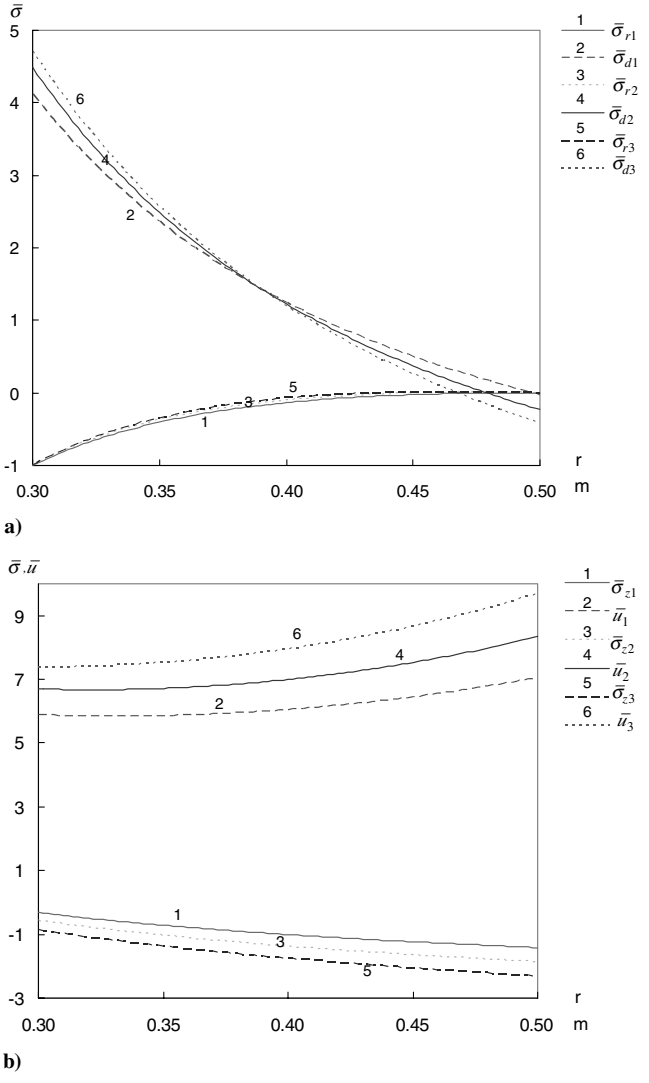

Fig. 2 Effects of coefficient e_0 on a) radial and circumferential stresses and b) axial stress and radial displacement.

According to [19,20], the stress–strain transfer ratio ξ and compositional distribution exponent M can be taken to be 4500 MPa and 0.5, respectively. From Eqs. (9), (35), and (36), the material coefficients of the functionally graded material are found to be $e_0 = 460$ GPa, $e_1 = 1.2531185$, $e_2 = -4.1770615$ 1/m, $\alpha_0 = 7.4 \times 10^{-6}$/K, $\alpha_1 = -1.3333378$, and $\alpha_2 = 4.4444593$ 1/m. Poisson's ratio of the functionally graded material is taken to be the average value of that of TiC and Ni (i.e., $\nu = 0.324$).

Using Eqs. (25–28), dimensionless stress and radial displacement can be determined using the following equations:

$$\bar{\sigma}_r = \frac{\sigma_r}{p}, \qquad \bar{\sigma}_\theta = \frac{\sigma_\theta}{p}, \qquad \bar{\sigma}_z = \frac{\sigma_z}{p}, \qquad \bar{u} = \frac{uE_i}{pr_i} \tag{37}$$

These dimensionless quantities are given in Figs. 1a and 1b and are indicated with the subscript capital A followed by the subscripts 2 or 5, standing for $n = 2$ and $n = 5$ in Eq. (14). Using Eqs. (32), (33), and (37) and taking $N = 300$, the results obtained from the numerical solution are also depicted in Figs. 1a and 1b and represented with the capital subscript N. To evaluate the difference in deformation and stress between varying and constant material properties, the thick-walled cylindrical vessel of constant Young's modulus and thermal expansion coefficient with the same geometric sizes and loads is also considered here. Young's modulus and thermal expansion coefficient of the cylindrical vessel are taken to be the average values of those at the inner and outer surfaces of the cylindrical vessel made of the functionally graded material, and the obtained radial displacement and stresses are shown in Figs. 1a and 1b and are indicated with the subscript capital C.

It can be seen from Figs. 1a and 1b that Eqs. (25–28) produce accurate results and that the computations converge quickly. Even

Table 1 Comparison of stresses and radial displacement results

Stresses and displacement at r_i	Numerical solution ($N = 300$)	Proposed solution		Constant material properties
		$n = 2$	$n = 5$	
$\bar{\sigma}_r$	−1	−1 (0%)	−1 (0%)	−1 (0%)
$\bar{\sigma}_\theta$	4.40681	4.48965 (1.88%)	4.4163 (0.22%)	2.125 (51.78%)
$\bar{\sigma}_z$	−0.598345	−0.571353 (4.51%)	−0.595118 (0.54%)	−1.72941 (189.03%)
$\bar{u}$	6.63606	6.70077 (0.98%)	6.63512 (0.01%)	5.10324 (23.1%)

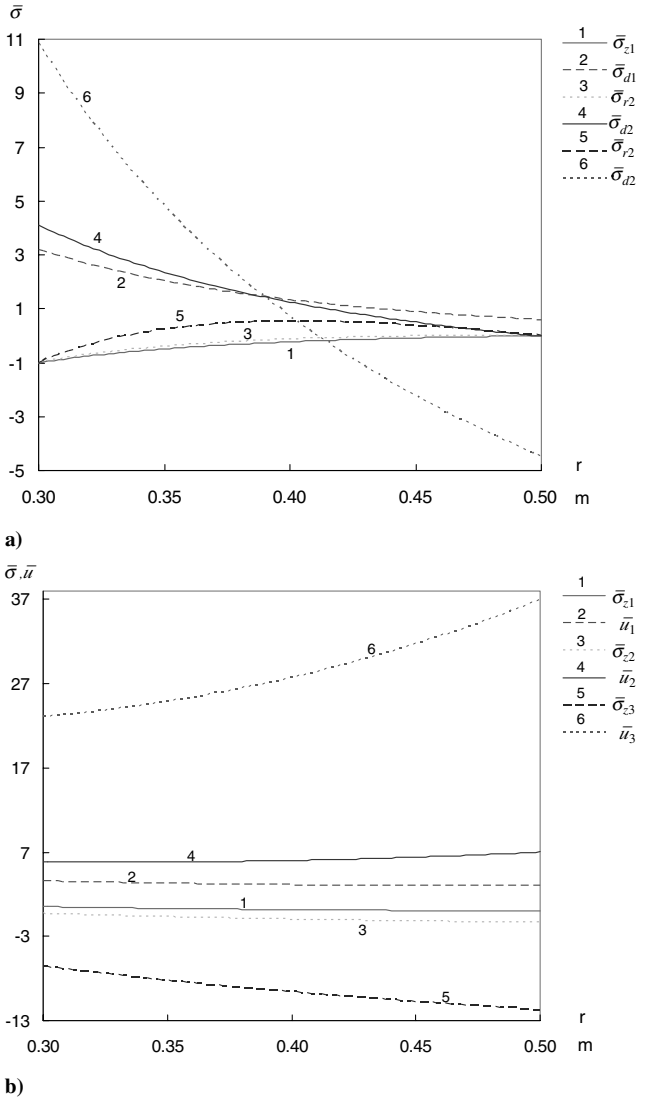

Fig. 3 Effects of coefficient e_1 on a) radial and circumferential stresses and b) axial stress and radial displacement.

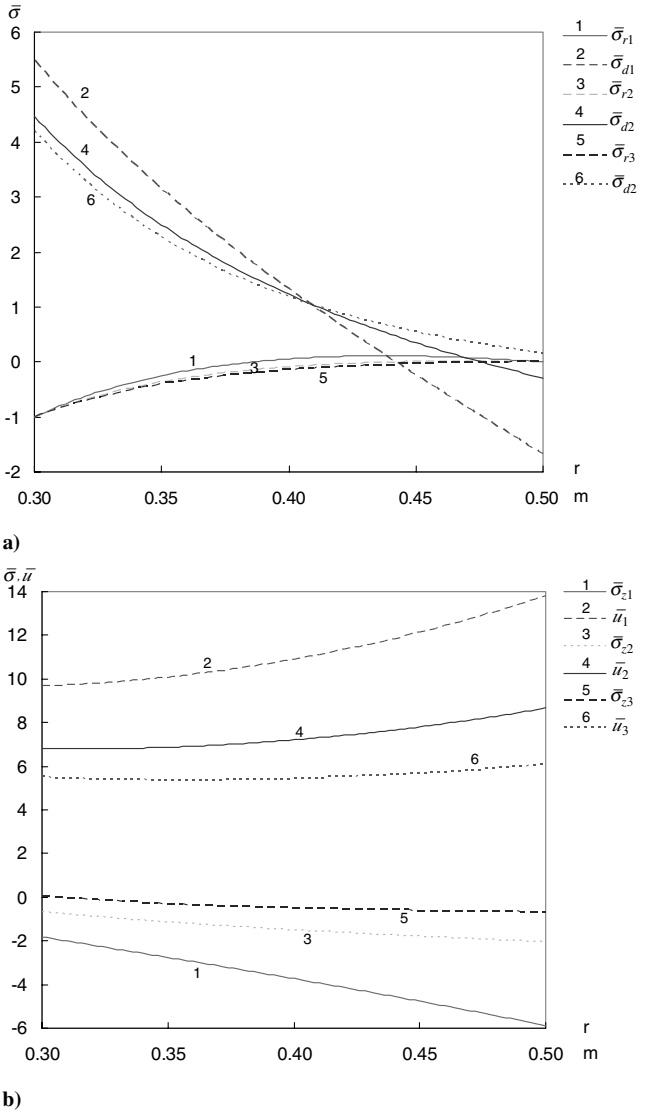

Fig. 4 Effects of coefficient e_2 on a) radial and circumferential stresses and b) axial stress and radial displacement.

using three terms in Eq. (14), the radial and axial stresses from the two different approaches are almost identical. Only small discrepancies of the circumferential stress and radial displacement in the region near the inner surface can be observed. To quantify the differences between the two approaches in comparison with the results obtained with average constant material properties, the radial displacement and stresses at the inner surface of the cylindrical vessel from different solutions are given in Table 1, in which the numbers in the parentheses indicate the errors relative to the numerical solution.

As can be seen from Table 1, when terms in Eq. (14) are increased from 3 ($n = 2$) to 6 ($n = 5$), the errors of the circumferential and axial stresses decrease from 1.88 and 4.51% to 0.22 and 0.54%, respectively, whereas that of the radial displacement drops from 0.98 to 0.01%. Even only taking three terms in Eq. (14), the maximum error of the radial displacement and stress results is 4.51% for $\bar{\sigma}_z$.

Unlike the axial stress from the functionally graded material, which varies along the thickness of the cylindrical vessel, the axial stress in the cylindrical vessel with constant Young's modulus and thermal expansion coefficient does not change along the radial direction, as shown in Fig. 1b. Also interesting are the distributions of the circumferential stress from varying and constant material properties models, which differ substantially. Compared with that from the constant material properties model, the circumferential stress from the varying material properties model is significantly higher at the inner surface but much lower at the outer surface, as shown in Fig. 1a. The error of circumferential stress at the inner surface from the two different material properties models is 51.78% at the inner surface. The radial displacement results from the two different material properties models are also noticeably different, as shown in Fig. 1b. Throughout the whole thickness of the cylindrical vessel, the radial displacement from the varying material properties model is always larger in comparison with the constant material properties model. At the inner surface of the cylindrical vessel, the error of the radial displacement from the two different material properties models is 23.1%.

To examine the effect of the coefficient e_0 used to define Young's modulus on deformation and stress results, all other coefficients affecting Young's modulus and thermal expansion coefficient are kept unchanged except e_0, which is set to be 360, 460, and 560 GPa, respectively. The corresponding dimensionless radial displacement and stress results are given in Figs. 2a and 2b, in which subscripts 1, 2, and 3 represent $e_0 = 360$, $e_0 = 460$, and $e_0 = 560$ GPa, respectively.

With the increase of the coefficient e_0, there are only minor changes of the compressive radial stress. The tensile circumferential stress becomes smaller in the region near the outer surface and greater in the region near the inner surface, as shown in Fig. 2a. Unlike the circumferential stress, the compressive axial stress is consistently greater through the whole thickness of the vessel with the increase of the coefficient e_0. It is noted that the differences in axial stress results due to different values of e_0 are greater toward the outer surface, as

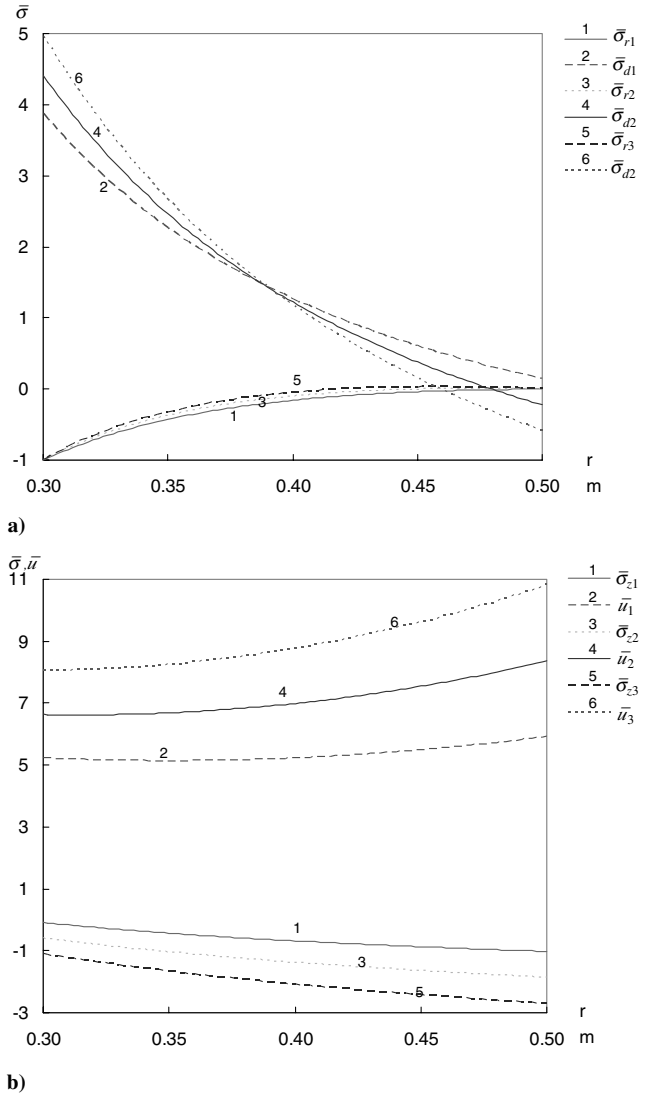

Fig. 5 Effects of coefficient α_0 on a) radial and circumferential stresses and b) axial stress and radial displacement.

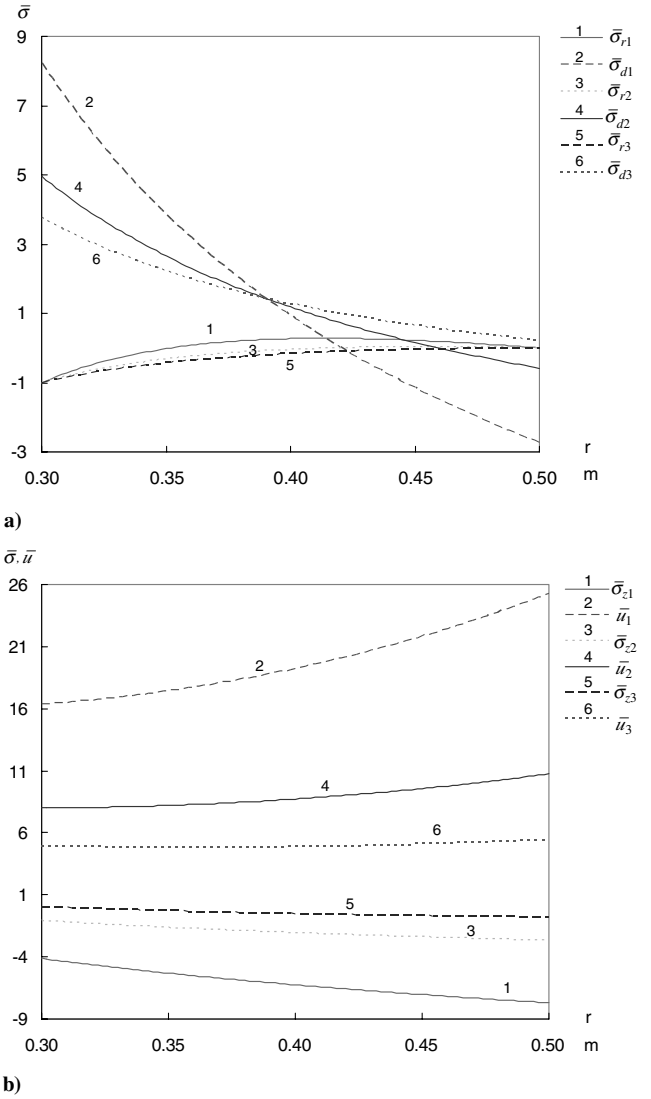

Fig. 6 Effects of coefficient α_1 on a) radial and circumferential stresses and b) axial stress and radial displacement.

shown in Fig. 2b. The radial displacement increases with the rise of the coefficient e_0 and the differences in radial displacement due to different values of e_0 become larger from the inner surface to the outer surface of the cylindrical vessel. It is also clear that the coefficient e_0 has the biggest effect on the radial displacement.

Fixing $e_0 = 460$ GPa and setting coefficient e_1 to be -1, 1, and 3, the calculated results are depicted in Figs. 3a and 3b, in which subscripts 1, 2, and 3 indicate $e_1 = -1$, $e_1 = 1$, and $e_1 = 3$, respectively.

As shown in Figs. 3a and 3b, different values of the coefficient e_1 have varying effect on the stresses and radial displacement results. When e_1 is increased from -1 to 1, only a small change is observed for all stress and radial displacement results. However, when e_1 is increased from 1 to 3, there are substantial variations in circumferential and axial stress as well as radial displacement results. The relative change of circumferential and axial stresses and radial displacement at the inner surface are 0.91, 0.85, and 2.33 when e_1 increases from -1 to 1. However, these figures reach 6.76, 6.88, and 17.23 when e_1 rises from 1 to 3.

Taking coefficient e_2 to be -2, -4, and -6 1/m, respectively, without changing the other coefficients, the variations of dimensionless stresses and radial displacement are shown in Figs. 4a and 4b. In the figures, subscripts 1, 2, and 3 indicate $e_2 = -2$, $e_2 = -4$, and $e_2 = -6$ 1/m, respectively.

It can be seen from the figures that the coefficient e_2 also greatly affects the circumferential and axial stresses and radial displacement in the cylindrical vessel. In each case, the relative change in circumferential and axial stresses and radial displacement that occur by varying the coefficient e_2 from -2 to -4 is larger than that which occurs by changing the coefficient e_2 from -4 to -6. In addition, the influences of coefficient e_2 on the circumferential and axial stresses and radial displacement at the outer surface are more obvious than at the inner surface.

The effects on how the thermal expansion coefficient affects the stress and deformation results in the cylindrical vessel are also evaluated. Taking coefficient α_0 in Eq. (9) to be 4.4×10^{-6}, 7.4×10^{-6}, and 10.4×10^{-6} 1/K and maintaining the value of the other coefficients, the obtained dimensionless stress and radial displacement results are given in Figs. 5a and 5b, in which subscripts 1, 2, and 3 indicate $\alpha_0 = 4.4 \times 10^{-6}$, $\alpha_0 = 7.4 \times 10^{-6}$, and $\alpha_0 = 10.4 \times 10^{-6}$ 1/K, respectively.

Accompanying the increase of coefficient α_0, little change is noted for the radial stress, as shown in Fig. 5a. The circumferential stress increases in the region closer to the inner surface and decreases in the region of the outer surface. The compressive axial stress and radial displacement increase with the rise of coefficient α_0. The relative variations of stress and radial displacement are, to a certain degree, proportional to the change of coefficient α_0. It is noticeable that among all results obtained, the influence of coefficient α_0 on the radial displacement is the most significant.

The effect of coefficient α_1 on deformation and stress is investigated by setting its values to be 0, -1, and -2, respectively.

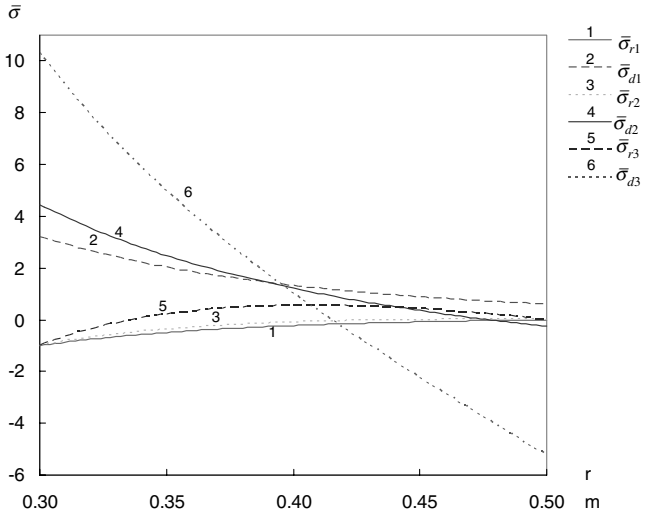

a)

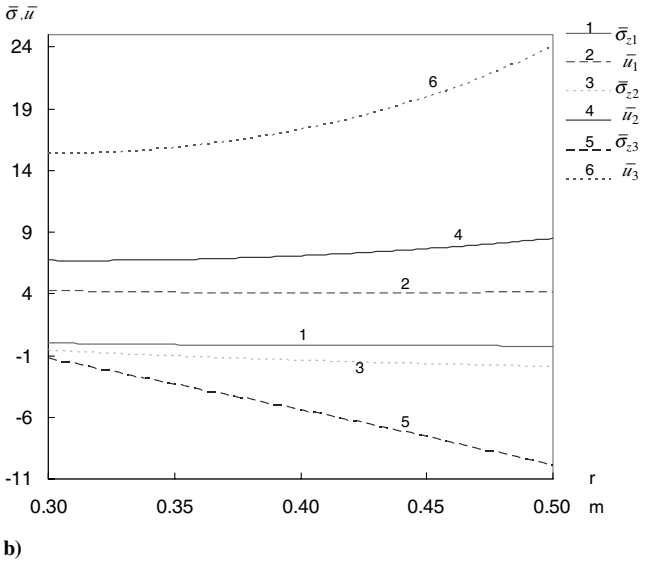

b)

Fig. 7 Effects of coefficient α_2 on a) radial and circumferential stresses and b) axial stress and radial displacement.

The calculated dimensionless stresses and radial displacement results are depicted in Figs. 6a and 6b, in which subscripts 1, 2, and 3 indicate $\alpha_1 = 0$, $\alpha_1 = -1$, and $\alpha_1 = -2$, respectively.

It can be observed that the variation of α_1 from 0 to -1 has a bigger effect on the circumferential and axial stresses and radial displacement than the change of α_1 from -1 to -2. When α_1 varies from -1 to -2, the circumferential stress, axial stress, and radial displacement at the inner surface are changed by 1.2, 1.1, and 3.1, respectively. However, when α_1 is changed from 0 to -1, the changes of the same results are increased to 3.4, 3, and 8.3, respectively. The effect of α_1 on the axial stress and radial displacement at the outer surface is more significant than at the inner surface.

Finally, the influence of the coefficient α_2 on deformation and stress in the cylindrical vessel is also evaluated. For this, the coefficient α_2 is set to be 1.5, 4.5, and 7.5 1/m and all other coefficients are kept unchanged. The obtained dimensionless stresses and radial displacement results are shown in Figs. 7a and 7b, in which subscripts 1, 2, and 3 indicate $\alpha_2 = 1.5$, $\alpha_2 = 4.5$, and $\alpha_2 = 7.5$ 1/m, respectively.

When coefficient α_2 is increased from 1.5 to 4.5 1/m, small changes are observed for all stresses and radial displacement results. However, when coefficient α_2 increases from 4.5 to 7.5 1/m, bigger changes of the circumferential and axial stresses and radial displacement results are apparent. The influence of coefficient α_2 on the circumferential stress at the inner and outer surfaces is similar. However, it has more obvious effect on the axial stress and radial displacement results at the outer surface than at the inner surface, as shown in Fig. 7b.

Conclusions

This study provides a new, accurate, and efficient analytical solution to predict deformations and stresses in thick-walled cylindrical vessels that have a varying Young's modulus and thermal expansion coefficient and are subjected to internal pressure and uniform temperature change. A number of conclusions can be drawn as follows:

1) For the cylindrical vessel made of a particular functionally graded material, the deformation and stress results obtained from the proposed method in comparison with a numerical-based approach demonstrate that the analytical solution is numerically accurate and computationally efficient.

2) The results show that the deformations and stresses of functionally graded cylindrical vessels behave quite differently from those with constant material properties. Therefore, the proposed analytical solution provides a robust and adequate solution to predict the deformations and stresses in functionally graded cylindrical vessels. Also, this method may be easily implemented and applied to practical design and analysis procedures.

3) In the parametric study of the effect of material properties, all material coefficients of Young's modulus and thermal expansion coefficient greatly influence the deformations and stress results. Careful consideration in choosing these material coefficients for the design of a proper functionally graded material can obviously improve the performance of thick-walled cylindrical vessels.

References

[1] Bland, D. R., "Elastoplastic Thick-Walled Tubes of Work-Hardening Material Subject to Internal and External Pressures and to Temperature Gradients," *Journal of the Mechanics and Physics of Solids*, Vol. 4, No. 4, 1956, pp. 209–229. doi:10.1016/0022-5096(56)90030-8

[2] Gao, X. L., "An Exact Elastoplastic Solution for an Open-Ended Thick-Walled Cylinder of Strain-Hardening Material," *International Journal of Pressure Vessels and Piping*, Vol. 52, No. 1, 1992, pp. 129–144. doi:10.1016/0308-0161(92)90064-M

[3] Gao, X. L., "An Exact Elastoplastic Solution for a Closed-End Thick-Walled Cylinder of Elastic Linear-Hardening Material in Large Strains," *International Journal of Pressure Vessels and Piping*, Vol. 56, No. 3, 1993, pp. 331–350. doi:10.1016/0308-0161(93)90004-D

[4] Durban, D., and Kubi, M., "A General Solution for the Pressurized Elastoplastic Tube," *Journal of Applied Mechanics*, Vol. 59, No. 1, 1992, pp. 20–26.

[5] Bonn, R., and Haupt, P., "Exact Solutions for Large Elastoplastic Deformations of a Thick-Walled Tube Under Internal Pressure," *International Journal of Plasticity*, Vol. 11, No. 1, 1995, pp. 99–118. doi:10.1016/0749-6419(94)00040-9

[6] Sayir, M. B., and Motavalli, M., "Fibre-Reinforced Laminated Composite Tubes with Free Ends Under Uniform Internal Pressure," *Journal of the Mechanics and Physics of Solids*, Vol. 43, No. 11, 1995, pp. 1691–1725. doi:10.1016/0022-5096(95)00055-N

[7] Kandil, A., El-Kady, A. A., and El-Kafrawy, A., "Transient Thermal Stress Analysis of Thick-Walled Cylinders," *International Journal of Mechanical Sciences*, Vol. 37, No. 7, 1995, pp. 721–732. doi:10.1016/0020-7403(94)00105-S

[8] Kandil, A., "Analysis of Thick-Walled Cylindrical Pressure Vessels Under the Effect of Cyclic Internal Pressure and Cyclic Temperature," *International Journal of Mechanical Sciences*, Vol. 38, No. 12, 1996, pp. 1319–1332. doi:10.1016/0020-7403(96)00001-X

[9] Zervos, A., Papanastasiou, P., and Vardoulakis, I., "Modelling of Localisation and Scale Effect in Thick-Walled Cylinders with Gradient Elastoplasticity," *International Journal of Solids and Structures*, Vol. 38, Nos. 30–31, 2001, pp. 5081–5095. doi:10.1016/S0020-7683(00)00337-1.

[10] Zhao, W., Seshadri, R., and Dubey, R. N., "On Thick-Walled Cylinder

Under Internal Pressure," *Journal of Pressure Vessel Technology*, Vol. 125, No. 3, 2003, pp. 267–273. doi:10.1115/1.1593082

[11] Finot, M., and Suresh, S., "Small and Large Deformation of Thick and Thin-Film Multi-Layers: Effects of Layer Geometry, Plasticity and Compositional Gradients," *Journal of the Mechanics and Physics of Solids*, Vol. 44, No. 5, 1996, pp. 683–721. doi:10.1016/0022-5096(96)84548-0

[12] Afsar, A. M., and Sekine, H., "Optimum Material Distributions for Prescribed Apparent Fracture Toughness in Thick-Walled FGM Circular Pipes," *International Journal of Pressure Vessels and Piping*, Vol. 78, No. 7, 2001, pp. 471–484. doi:10.1016/S0308-0161(01)00061-8

[13] Ma, L. S., and Wang, T. J., "Nonlinear Bending and Post-Buckling of a Functionally Graded Circular Plate Under Mechanical and Thermal Loadings," *International Journal of Solids and Structures*, Vol. 40, Nos. 13–14, 2003, pp. 3311–3330. doi:10.1016/S0020-7683(03)00118-5

[14] Liew, K. M., Kitipornchai, S., Zhang, X. Z., and Lim, C. W., "Analysis of the Thermal Stress Behaviour of Functionally Graded Hollow Circular Cylinders," *International Journal of Solids and Structures*, Vol. 40, No. 10, 2003, pp. 2355–2380. doi:10.1016/S0020-7683(03)00061-1

[15] Chen, Y. Z., "Stress Intensity Factors in a Finite Cracked Cylinder Made of Functionally Graded Materials," *International Journal of Pressure Vessels and Piping*, Vol. 81, No. 12, 2004, pp. 941–947. doi:10.1016/j.ijpvp.2004.05.008

[16] You, L. H., Zhang, J. J., and You, X. Y., "Elastic Analysis of Internally Pressurized Thick-Walled Spherical Pressure Vessels of Functionally Graded Materials," *International Journal of Pressure Vessels and Piping*, Vol. 82, No. 5, 2005, pp. 347–354. doi:10.1016/j.ijpvp.2004.11.001

[17] You, L. H., Tang, Y. Y., Zhang, J. J., and Zheng, C. Y., "Numerical Analysis of Elastic–Plastic Rotating Disks with Arbitrary Variable Thickness and Density," *International Journal of Solids and Structures*, Vol. 37, No. 52, 2000, pp. 7809–7820. doi:10.1016/S0020-7683(99)00308-X

[18] Abramowitz, M., and Stegun, A. I. (eds.), *Handbook of Mathematical Functions*, 5th ed., U.S. Government Printing Office, Washington, DC, 1966.

[19] Zhang, X.-H., Han, J.-C., Du, S.-Y., and Wood, J. V., "Microstructure and Mechanical Properties of TiC–Ni Functionally Graded Materials by Simultaneous Combustion Synthesis and Compaction," *Journal of Materials Science*, Vol. 35, No. 8, 2000, pp. 1925–1930. doi:10.1023/A:1004714402128

[20] Cho, J. R., and Ha, D. Y., "Averaging and Finite-Element Discretization Approaches in the Numerical Analysis of Functionally Graded Materials," *Materials Science and Engineering A*, Vol. 302, No. 2, 2001, pp. 187–196. doi:10.1016/S0921-5093(00)01835-9

A. Palazotto
Associate Editor